ELSEVIER

Biophysical Chemistry 105 (2003) 89–104

Biophysical Chemistry

www.elsevier.com/locate/bpc

Preferred conformations of cyclic Ac–Cys–Pro–Xaa–Cys–NHMe peptides: a model for chain reversal and active site of disulfide oxidoreductase

Hae Sook Park[a], Choonmi Kim[b], Young Kee Kang[c,*]

[a]*Department of Radiotechnology, Cheju-halla College, Cheju 690-708, South Korea*
[b]*College of Pharmacy, Ewha Womans University, Seoul 120-750, South Korea*
[c]*Department of Chemistry, Chungbuk National University, Cheongju, Chungbuk 361-763, South Korea*

Received 12 April 2003; received in revised form 28 April 2003; accepted 28 April 2003

Abstract

The conformational study on cyclic Ac–Cys–Pro–Xaa–Cys–NHMe (Ac–CPXC–NHMe; X = Ala, Val, Leu, Aib, Gly, His, Phe, Tyr, Asn and Ser) peptides has been carried out using the Empirical Conformational Energy Program for Peptides, version 3 (ECEPP/3) force field and the hydration shell model in the unhydrated and hydrated states. This work has been undertaken to investigate structural implications of the CPXC sequence as the chain reversal for the initiation of protein folding and as the motif for active site of disulfide oxidoreductases. The backbone conformation DAAA is commonly the most feasible for cyclic CPXC peptides in the hydrated state, which has a type I β-turn at the Pro–Xaa sequence. The proline residue and the hydrogen bond between backbones of two cystines as well as the formation of disulfide bond appear to play a role in stabilizing this preferred conformation of cyclic CPXC peptides. However, the distributions of backbone conformations and β-turns may indicate that the cyclic CPXC peptide seems to exist as an ensemble of β-turns and coiled conformations in aqueous solution. The intrinsic stability of the cyclic CPXC motif itself for the active conformation seems to play a role in determining electrochemical properties of disulfide oxidoreductases.

Keywords: Cyclic CPXC peptides; Conformational study; β-Turns; Hydration; Disulfide oxidoreductase

1. Introduction

Disulfide bonds have been known to play a role in stabilizing the structure and folding of proteins [1,2]. The formation of disulfide bonds seems to be facilitated by decreasing the entropy of the unfolded state [3] and by providing the favorable local interactions in the folded state [4].

Many experimental and theoretical studies have been attempted on chain reversals because of their involvement in the initiation of protein folding [5]. Cyclic peptides with a disulfide bond have been used as models for chain reversals because they can exist with a higher population of ordered conformations in solution [6]. In particular, the

*Corresponding author. Tel.: +82-43-261-2285; fax: +82-43-273-8328.
E-mail address: ykkang@chungbuk.ac.kr (Y.K. Kang).

0301-4622/03/$ - see front matter © 2003 Elsevier B.V. All rights reserved.
doi:10.1016/S0301-4622(03)00139-X

cyclic tetrapeptides of sequence Cys–Pro–Xaa–Cys (or CPXC) have been studied to estimate their propensity to form β-turns [6–10].

The Pro–Xaa sequence has been known to have high proportions to form β-turns at the second and third positions [11]. The Cys residue shows a significant preference to be at the first position of a type I β-turn [12,13]. The Pro residue is the most strongly preferred amino acid at the second position of both types I and II β-turns [11–13], which are due to the inherent restriction on torsion angle ϕ for the N–C^{α} bond of Pro to approximately $-60°$. X-ray diffraction and NMR experiments on cyclic CPXC peptides support that the type I β-turn is the most preferred conformation for their Pro–Xaa sequences [6–10].

The CXXC sequence is known to be a motif located at active sites of protein disulfide oxidoreductases [14,15]. Crystal and NMR structures of oxidoreductases such as thioredoxin [16–19], glutaredoxin [20], thioredoxin reductase [21], T4 glutaredoxin [22], thioltransferase [23], DsbA [24,25], the DsbA homolog (TcpG) [26], DsbA mutants [24,25], and the hyperthermostable oxidoreductase from *Pyrococcus furiosus* [27] do not show significant differences in their conformations of the active site, in which the disulfide bonds are in the right-handed hook conformation with the disulfide torsion angle χ_{SS} of approximately $+80°$ [1]. These structural studies exhibit that the N-terminal cystine of the active site is located in a loop between β-strand and α-helix, while the C-terminal cystine is in the first turn of the α-helix (hereafter, the first and fourth cystines of the CPXC sequence will be denoted as Cys1 and Cys4, respectively). Despite this similarity, however, the reduction potentials appear to strongly depend on the XX dipeptide sequence [15,28].

In particular, glutaredoxin, thioltransferase, DsbA and the thermostable oxidoreductase from *Pyrococcus furiosus* have the CPXC sequence of the active site. X-ray structures of proteins indicate that Pro is frequently found at the N-terminus of α-helices [29–31]. The higher preference of proline at the beginning of α-helix appears to be due to the favored local interactions between two residues preceding proline and no disturbance in hydrogen bonds of α-helix by proline [32].

In the present study, we have carried out a conformational study for cyclic CPXC peptides in the unhydrated and hydrated states, in order to figure out factors to influence on the intrinsic conformational preference and the stability of the CPXC sequence as a model for chain reversal and active site of disulfide oxidoreductase.

2. Methods

The nomenclature and conventions used follow the recommendations of the IUPAC-IUB Commission on Biochemical Nomenclature [33,34]. The calculations were carried out on cyclic Ac–CPXC–NHMe tetrapeptides (X = Ala, Val, Leu, Aib, Gly, His, Phe, Tyr, Asn and Ser) in the unhydrated and hydrated states. The structures of peptides [6–10] and disulfide oxidoreductases [23–27] containing the CPXC sequence were examined by X-ray diffraction and/or NMR experiment. The thiol/disulfide equilibrium of the sequences with X = Val, Aib, Gly, Phe, Asn and Ser was studied with automated HPLC measurements [6].

Conformational energy calculations were carried out using the ECEPP/3 (Empirical Conformational Energy Program for Peptides, version 3) force field [35], in which the total conformational energy (E_{tot}) is the sum of the electrostatic energy (E_{es}), the nonbonded energy (E_{nb}), the torsional energy (E_{tor}), the cystine torsional energy (E_{cystr}), and the loop energy for the S–S bond (E_{loop}). The hydrogen bond energy is included in the nonbonded energy component. The hydration shell model improved by Kang et al. [36–39] was used to calculate the hydration free energy ($\Delta\Delta G_{hyd}$) of each conformation of the peptides in the hydrated state, where the hydration free energy was obtained as the sum of the free energy proportional to the water-accessible volume for each united group and the polarization free energy between polar groups. The total free energy (ΔG_{tot}) of each hydrated conformation was calculated using the sum of the total conformational energy (ΔE_{tot}) and the hydration free energy ($\Delta\Delta G_{hyd}$).

Each conformation of the peptide was denoted in terms of a conformational letter code of Zimmerman et al. [40] that was assigned to each

residue specifying its location on a backbone $\phi-\psi$ map. Conformational states for side-chain torsion angle χ^1 with respect to a threefold rotational barrier having minima near 60°, 180° and −60° are denoted by the lowercase letters g^+, t and g^-, respectively. The torsion angle χ^1 indicated by each letter extended over a range of 120°, i.e. g^+ denotes $0° \leqslant \chi^1 < 120°$, etc.

The starting conformations for minimization of the dipeptide Ac–Pro–Xaa–NHMe in the unhydrated state were generated by combining energy minima of Ac–Pro–NHMe and Ac–Xaa–NHMe. Four minimum-energy conformations *t*Au, *t*Fu, *c*Au and *c*Fu of Ac–Pro–NHMe with the up-puckering [35] were used for generation of starting conformations, where *t* and *c* represent the *trans* and *cis* Ac–Pro peptide bond. Based on X-ray structures of proline-containing sequences of proteins [41], only the up-puckered conformations are included. Because the relative energy of the conformation *t*Cu of proline in Ac–Pro–NHMe is found to be not too high (1.93 kcal/mol) and the conformation D*t*Cu of Ac–Ala–Pro–NHMe has relatively a low conformational energy of 1.88 kcal/mol [35], the conformation *t*Cu of proline in Ac–Pro–NHMe is additionally included in generating starting conformations.

In the case of Xaa = Ala, Val, Leu, Gly, Phe, Tyr and Ser, their minima with $\Delta E_{tot} < 5$ kcal/mol reported in Ref. [42] were included for the generation of starting points. On the other hand, energy minima of Ac–Xaa–NHMe for Xaa = His and Asn with $\Delta E_{tot} < 3$ kcal/mol were used as the starting conformations for minimization, because the most of their conformations have $\Delta E_{tot} < 3$ kcal/mol and appear to be large enough [42]. Ac–Aib–NHMe has nine minimum conformations, optimized from all energy minima of Ac–Ala–NHMe in Ref. [42], of which two conformations have $\Delta E_{tot} < 3$ kcal/mol and other seven conformations have the relative energies between 3 and 10 kcal/mol. So all nine conformations for Ac–Aib–NHMe were used for the generation of starting conformations. The backbone conformation A* was found to be the most probable for Ac–Aib–NHMe. Energy minima of Ac–Pro–Xaa–NHMe with $\Delta E_{tot} < 5$ kcal/mol were used to generate starting conformations of cyclic Ac–CPXC–NHMe by combining feasible conformations of cystine residue. The cutoff of 3 kcal/mol for ΔE_{tot} employed in generating starting points for minimization was suggested to be reasonable for conformational searching of penta- and hexa-peptides with the buildup procedure [43,44]. The five minimum-energy backbone conformations of Ac–Ala–NHMe [42] and two backbone conformations of X-ray structures of cyclic Ac–CPVC–NHMe and Ac–CPSC–NHMe [6] were combined with three *t*, g^+ and g^- conformations for the side-chain torsion angle χ^1 of cystine residue to give 21 feasible conformations for cystine residue. Side-chains of Cys, Pro and X residues as well as acetyl and methyl amide end groups were taken to be in their uncharged forms to simulate the effect of ionic shielding.

A quasi-Newton algorithm SUMSL (Secant-type Unconstrained Minimization problem So-Lver) [45] was used for energy minimization in the unhydrated state and free energy minimization in the hydrated state. All torsion angles of the backbone, side-chains, and end-groups of peptides were allowed to move during minimization. Minimized conformations of cyclic Ac–CPXC–NHMe peptides in the unhydrated state were used as their starting conformations for minimization in the hydrated state.

Four residues of cyclic Ac–CPXC–NHMe peptides are defined as residues $i+1$, $i+2$, $i+3$ and $i+4$, respectively. The N-terminal group Ac- and the C-terminal group –NHMe are defined as the residue i and $i+5$, respectively. The quantity h is the $O_{i+1}\cdots N_{i+4}$ distance, which is used to define the hydrogen bonds of backbone [11]. In this work, the hydrogen bond is defined when the distance between hydrogen and hydrogen-acceptor is $\leqslant$2.4 Å. This criterion was applied to all hydrogen bonds for backbone, side-chains and end-groups. The quantity R is the $C^{\alpha}_{i+1}\cdots C^{\alpha}_{i+4}$ distance. A β-turn is defined as a conformation in which $R \leqslant 7$ Å, and various types of β-turn can be defined by the backbone torsion angles ϕ and ψ of the second and third residues of four consecutive residues [11]. Since the types I and III have no distinct structural characteristics and form a continuous distribution on a $\phi-\psi$ map of protein

structures, the type III was eliminated as a distinct category [46].

The normalized statistical weight w_i of the conformation i was calculated according to the Boltzmann equation [11] given by

$$w_i = (1/Z)\exp\left(-\Delta G_i/RT\right) \quad (1)$$

where

$$Z = \sum_{i=1}^{n} \exp(-\Delta G_i/RT) \quad (2)$$

Here, ΔG_i is $\Delta E_{\mathrm{tot},i}$ or $\Delta G_{\mathrm{tot},i}$ in the unhydrated or hydrated states, respectively, R is the gas constant and T is the absolute temperature. The summation was taken over all n low energy or free energy minima shown in Table 1.

Vicinal coupling constants ^3J were computed by using the expression

$$^3J = A\cos^2\theta + B\cos\theta + C \quad (3)$$

where $\theta = |\phi - 60°|$ for $^3J_{\mathrm{HN}\alpha}$, $\theta = \chi^1 - 120°$ for $\mathrm{H}\beta_2$, $\theta = \chi^1$ for $\mathrm{H}\beta_3$. Values used for A, B and C in Eq. (3) are 6.4, −1.4 and 1.9 Hz for $^3J_{\mathrm{HN}\alpha}$ [47], and 9.5, −1.6 and 1.8 Hz for $^3J_{\alpha\beta}$ [48].

The statistically weighted average value of any conformation-dependent quantity q (i.e. h, R and ^3J) was calculated by the following equation using the statistical weight w_i of Eq. (1);

$$\langle q\rangle = \sum_{i=1}^{n} w_i q_i \quad (4)$$

The probability P_i of occurrence of the type i β-turns was computed as the sum of corresponding statistical weights w_is. All thermodynamic quantities were calculated for $T = 298.15$ K.

3. Results and discussion

3.1. General conformational properties

Table 1 shows the number of starting and minimized conformations of cyclic CPXC peptides in the unhydrated and hydrated states. Starting conformations of each peptide in the hydrated state are the corresponding optimized conformations in the unhydrated state. The statistically averaged values of $\langle h\rangle$, $\langle R\rangle$, and the probability P of β-turn conformation for the Pro–Xaa sequence at positions $i+2$ and $i+3$ of a β-turn are included in Table 1.

Table 1
Conformational properties of cyclic Ac–Cys–Pro–Xaa–Cys–NHMe peptides in the unhydrated and hydrated states

Xaa	State[a]	No. of conf.[b]		Conf. properties[c]		β-Turn prob.[d]
		m	n	$\langle h\rangle$	$\langle R\rangle$	P
Ala	Unh	11 014	25	2.90	5.25	1.00
	Hyd	25	20	3.00	5.30	1.00
Val	Unh	14 094	31	2.89	5.24	1.00
	Hyd	31	26	2.96	5.28	1.00
Leu	Unh	27 752	60	2.89	5.24	1.00
	Hyd	60	50	3.01	5.30	1.00
Aib	Unh	4407	38	2.87	5.20	1.00
	Hyd	38	32	2.99	5.34	1.00
Gly	Unh	11 442	56	2.90	5.26	1.00
	Hyd	56	44	3.10	5.35	1.00
His	Unh	46 669	100	2.99	5.29	1.00
	Hyd	100	77	3.06	5.32	1.00
Phe	Unh	24 206	38	2.96	5.29	1.00
	Hyd	38	26	2.98	5.31	1.00
Tyr	Unh	38 731	77	2.96	5.29	1.00
	Hyd	77	54	3.00	5.32	1.00
Asn	Unh	37 414	61	2.94	5.27	1.00
	Hyd	61	43	3.14	5.34	1.00
Ser	Unh	62 552	100	2.93	5.27	1.00
	Hyd	100	85	3.08	5.33	1.00

[a] Unh and Hyd correspond to unhydrated and hydrated states, respectively.

[b] m and n correspond to the number of starting and optimized conformations, respectively; see the text. Numbers of minimized conformations correspond to those with $\Delta E_{\mathrm{tot}} \leqslant 5$ kcal/mol in the unhydrated state and $\Delta G_{\mathrm{tot}} \leqslant 5$ kcal/mol in the hydrated state.

[c] Conformational properties. The quantity h is the $O_{\mathrm{cys1}}\cdots N_{\mathrm{cys4}}$ distance of the backbone. The quantity R is the $C^{\alpha}_{\mathrm{cys1}}\cdots C^{\alpha}_{\mathrm{cys4}}$ distance.

[d] β-Turn probabilities of P is defined for the Pro–Xaa sequence.

The value of $\langle h \rangle$ is a measure of the formation of backbone-to-backbone hydrogen bond in some β-turn structures, and the value of $\langle R \rangle$ is a criterion to distinguish the β-turn from other conformations. The values of 5.20–5.29 Å for $\langle R \rangle$ of the Pro–Xaa sequence in the unhydrated state is a little smaller than those of 5.28–5.33 Å in the hydrated state. This indicates that the conformations in the unhydrated state are more compact than those in the hydrated state. In particular, the probabilities P to form β-turns are all 1.00 in both states. It indicates that all peptides have the β-turn structures for the Pro–Xaa sequence. The number of minimized conformations with $\Delta G_{tot} \leqslant 5$ kcal/mol for each cyclic CPXC peptide in the hydrated state is less than those with $\Delta E_{tot} \leqslant 5$ kcal/mol in the unhydrated state. It shows that hydration play a role in determining the conformational preference of the peptide in the hydrated state. Thus, the differences in values of $\langle R \rangle$ and $\langle h \rangle$ may suggest that the Pro–Xaa sequence plays a role in determining the conformation of peptide backbone.

3.2. Preferred conformations and population of backbone conformations

Table 2 lists the low energy conformations and their energies of cyclic CPXC peptides with relative free energies (ΔG_{tot}) $\leqslant 1$ kcal/mol in the hydrated state. Each conformation is designated by its backbone conformation and torsion angle χ^1. Preferred conformations of each cyclic CPXC peptide, which have different conformations for backbone and side-chain torsion angle χ^1 with $\Delta G_{tot} \leqslant 1$ kcal/mol, are designated in parentheses of the first column for each peptide in Table 2 (e.g. A1, A2 and A3 for cyclic Ac–CPAC–NHMe).

The lowest free energy backbone conformation of cyclic CPXC peptide is DAAA except for CPFC and CPYC peptides. Its statistical weight is 0.133 (X = Ser) to 0.498 (X = Val). The conformation DAAA appears to be stabilized by a hydrogen bond between the C=O of Cys1 residue and the N–H of Cys4 residue with the distance r(N–H···O) = 1.97–2.01 Å. Although the backbone conformation DAAA is the second and third lowest free energy conformations for cyclic CPFC and CPYC peptides, respectively, it seems to be energetically comparable to the most probable conformation DAAC.

The second lowest free energy backbone conformation is DAAC except for X = Leu, Aib, Phe, Tyr and Ser, whose statistical weight is 0.167 (X = His) to 0.350 (X = Val). In particular, this backbone conformation DAAC is the lowest free energy conformation for cyclic CPFC and CPYC peptides, whose statistical weights are 0.358 and 0.178, respectively. However, the backbone conformation DAAC appears to be feasible for cyclic CPLC and CPSC peptides, whose statistical weights are 0.199 and 0.059, respectively. In the case for X = Aib, the backbone conformation DAAC is the sixth lowest free energy conformation, whose statistical weight is 0.059. This backbone conformation DAAC has two hydrogen bonds, one as the same as for the conformation DAAA and another between the N–H of carboxylic end-group and the C=O of Xaa residue. For both preferred backbone conformations DAAA and DAAC, the conformations of side-chain χ^1 are g^+ for X = Ala and Aib, t for X = Val, and g^- for X = Leu, His, Phe, Tyr, Asn and Ser.

In the case of the cyclic CPAibC peptide, the backbone conformation of the second lowest free energy conformation is DCA*C, which seems to be stabilized by two hydrogen bonds between the C=O of Cys1 residue and the N–H of Cys4 residue and between the C=O of Aib residue and the N–H of NHMe end-group with the distances r(N–H···O) equal to 2.24 and 2.12 Å, respectively. The methyl group attached to the C^{α} of Aib residue appears to play a role in stabilizing this backbone conformation because the backbone conformation CA* for the Pro–X sequence is feasible only for the Aib peptide (Table 2). It should be noted that the backbone conformation A* was found to be the most probable for Ac–Aib–NHMe (Section 2).

The backbone conformation DABA is the fourth, third, third and fourth lowest free energy conformations of cyclic CPAC, CPGC, CPFC and CPSC peptides, respectively, which seems to be stabilized by the hydrogen bond between the C=O of Cys1 residue and the N–H of Cys4 residue with the distance r(N–H···O) equal to 2.00–2.05 Å.

Table 2
Conformations and energies of cyclic Ac–Cys–Pro–Xaa–Cys–NHMe peptide with $\Delta G_{tot} \leqslant 1$ kcal/mol in the hydrated state

Conf.[a]	ΔG_{tot}[b]	ΔE_{tot}[c]	ΔE_{es}[d]	ΔE_{nb}[e]	ΔE_{tor}[f]	ΔE_{cystr}[g]	ΔE_{loop}[h]	$\Delta\Delta G_{hyd}$[i]	w[j]	β-Turn[k]
Ac–Cys–Pro–Ala–Cys-NHMe										
D*t*AA*g*$^+$A*g*$^-$(A1)	0.00	0.00	0.00	0.00	0.00	0.00	0.00	0.00	0.365	I
D*t*AA*g*$^+$C*g*$^-$(A2)	0.26	1.24	−0.58	1.57	0.36	−0.03	−0.08	−0.98	0.235	I
D*t*AA*g*$^+$A*g*$^-$	0.53	0.41	−0.10	0.26	−0.03	0.31	−0.02	0.12	0.151	I
D*t*AB*g*$^+$A*g*$^-$(A3)	0.66	0.93	−0.39	0.81	0.95	−0.15	−0.29	−0.27	0.119	I
Ac–Cys–Pro–Val–Cys–NHMe										
D*t*AA*t*A*g*$^-$(V1)	0.00	0.00	0.00	0.00	0.00	0.00	0.00	0.00	0.498	I
D*t*AA*t*C*g*$^-$(V2)	0.21	1.34	−0.58	1.73	0.43	−0.13	−0.13	−1.13	0.350	I
Ac–Cys–Pro–Leu–Cys–NHMe										
D*t*AA*g*$^-$A*g*$^-$(L1)	0.00	0.00	0.00	0.00	0.00	0.00	0.00	0.00	0.275	I
D*t*AA*t*A*g*$^-$(L2)	0.10	−0.05	−0.03	−0.05	−0.23	0.09	0.18	0.15	0.231	I
D*t*AA*g*$^-$C*g*$^-$(L3)	0.19	1.17	−0.48	1.57	0.24	−0.13	−0.04	−0.98	0.199	I
D*t*AA*t*C*g*$^-$(L4)	0.76	1.34	−0.55	1.88	0.02	−0.07	0.07	−0.58	0.076	I
Ac–Cys–Pro–Aib–Cys-NHMe										
D*t*AA*g*$^+$A*g*$^-$(B1)	0.00	0.00	0.00	0.00	0.00	0.00	0.00	0.00	0.295	I
D*t*CA***g*$^+$C*g*$^-$(B2)	0.34	2.58	−0.81	3.42	2.12	−1.49	−0.67	−2.24	0.176	II
D*t*AA*g*$^+$A*g*$^-$	0.36	0.41	−0.12	0.43	0.07	0.10	−0.07	−0.05	0.161	I
D*t*CA***g*$^+$C*g*$^-$	0.64	2.86	−0.97	3.88	2.07	−1.41	−0.70	−2.22	0.100	II
E*g*$^+$CA***g*$^+$C*g*$^-$(B3)	0.89	2.72	−0.73	2.75	1.60	−0.17	−0.73	−1.84	0.066	II
D*t*AAg$^+$C*g*$^-$(B4)	0.95	1.87	−0.58	2.20	0.67	−0.23	−0.20	−0.91	0.059	I
Ac–Cys–Pro–Gly–Cys–NHMe										
D*t*AAA*g*$^-$(G1)	0.00	0.00	0.00	0.00	0.00	0.00	0.00	0.00	0.304	I
D*t*AAC*g*$^-$(G2)	0.21	1.14	−0.54	1.61	0.29	−0.14	−0.07	−0.94	0.215	I
D*t*ABA*g*$^-$(G3)	0.58	0.90	−0.45	0.86	0.95	−0.19	−0.26	−0.32	0.114	I
D*t*AAC*g*$^-$	0.93	1.74	−0.66	2.26	0.32	−0.07	−0.10	−0.81	0.063	I
E*g*$^+$ADE*g*$^+$(G4)	0.95	2.93	0.86	3.16	0.56	−1.31	−0.35	−1.98	0.061	VII
Ac–Cys–Pro–His–Cys–NHMe										
D*t*AA*g*$^-$A*g*$^-$(H1)	0.00	0.00	0.00	0.00	0.00	0.00	0.00	0.00	0.229	I
D*t*AA*g*$^-$C*g*$^-$(H2)	0.19	1.22	−0.51	1.60	0.37	−0.14	−0.12	−1.03	0.167	I
D*t*AA*t*A*g*$^-$(H3)	0.49	0.60	0.17	0.33	−0.10	0.11	0.09	−0.11	0.100	I
D*t*AA*t*A*g*$^-$	0.78	0.79	0.06	0.67	0.08	−0.01	−0.02	−0.01	0.062	I
D*t*AA*g*$^-$A*g*$^-$	0.81	−0.20	0.09	−0.26	0.18	−0.09	−0.12	1.01	0.059	I
D*t*AA*t*C*g*$^-$(H4)	0.85	1.92	−0.49	2.14	0.39	−0.06	−0.06	−1.06	0.054	I
Ac–Cys–Pro–Phe–Cys–NHMe										
D*t*AA*g*$^-$C*g*$^-$(F1)	0.00	0.00	0.00	0.00	0.00	0.00	0.00	0.00	0.358	I
D*t*AA*g*$^-$A*g*$^-$(F2)	0.11	−1.03	0.35	−1.30	−0.37	0.14	0.15	1.15	0.295	I
D*t*AB*g*$^-$A*g*$^-$(F3)	0.48	−0.41	0.30	−1.30	0.66	−0.05	−0.01	0.89	0.159	I
D*t*AA*t*A*g*$^-$(F4)	0.82	−0.48	0.55	−0.96	−0.60	0.24	0.30	1.30	0.089	I
Ac–Cys–Pro–Tyr–Cys–NHMe										
D*t*AA*g*$^-$C*g*$^-$(Y1)	0.00	0.00	0.00	0.00	0.00	0.00	0.00	0.00	0.178	I
D*t*AA*g*$^-$C*g*$^-$	0.03	0.03	0.03	0.06	−0.04	0.00	−0.03	0.00	0.169	I
D*t*AA*g*$^-$A*g*$^-$(Y2)	0.07	−0.95	0.33	−1.34	−0.07	0.09	0.03	1.02	0.158	I
D*t*AA*g*$^-$A*g*$^-$	0.13	−0.95	0.39	−1.29	−0.27	0.11	0.11	1.08	0.144	I
D*t*AB*g*$^-$C*g*$^-$(Y3)	0.33	0.64	0.09	−0.22	1.09	−0.19	−0.13	−0.31	0.108	I
D*t*AA*t*A*g*$^-$(Y4)	0.71	−0.37	0.47	−0.87	−0.44	0.22	0.25	1.08	0.054	I
D*t*AA*t*A*g*$^-$	0.80	−0.41	0.48	−0.91	−0.48	0.22	0.27	1.21	0.047	I
D*t*AB*g*$^-$C*g*$^-$	0.97	1.18	0.37	0.25	0.74	−0.06	−0.13	−0.21	0.035	I
Ac–Cys–Pro–Asn–Cys–NHMe										
D*t*AA*g*$^-$A*g*$^-$(N1)	0.00	0.00	0.00	0.00	0.00	0.00	0.00	0.00	0.400	I
D*t*AA*g*$^-$C*g*$^-$(N2)	0.41	1.43	−0.38	1.64	0.42	−0.14	−0.11	−1.02	0.199	I

Table 2 *(Continued)*

Conf.[a]	ΔG_{tot}[b]	ΔE_{tot}[c]	ΔE_{es}[d]	ΔE_{nb}[e]	ΔE_{tor}[f]	ΔE_{cystr}[g]	ΔE_{loop}[h]	$\Delta\Delta G_{hyd}$[i]	w[j]	β-Turn[k]
Ac–Cys–Pro–Ser–Cys–NHMe										
D*t*AAg^-Ag^-(S1)	0.00	0.00	0.00	0.00	0.00	0.00	0.00	0.00	0.133	I
D*t*AAg^+Ag^-(S2)	0.05	−0.62	−0.48	−0.27	0.06	0.04	0.03	0.67	0.122	I
D*t*AAg^-Ag^-	0.14	−0.01	−0.05	−0.07	−0.03	0.04	0.10	0.15	0.106	I
D*t*AB*t*Ag^-(S3)	0.33	0.79	−0.39	0.90	0.61	−0.16	−0.16	−0.47	0.077	I
D*t*AAg^-Cg^-(S4)	0.48	1.34	−0.44	1.69	0.24	−0.13	−0.02	−0.86	0.059	I
D*t*AAg^+Ag^-	0.50	−0.40	−0.54	−0.23	0.34	0.02	0.01	0.91	0.057	I
D*t*AAg^+Cg^-(S5)	0.51	0.93	−0.91	1.61	0.44	−0.02	−0.18	−0.42	0.056	I
D*t*AAg^-Cg^-	0.63	1.34	−0.56	1.76	0.26	−0.11	−0.02	−0.71	0.046	I
D*t*AB*t*Cg^-(S6)	0.80	2.22	−0.55	2.49	0.81	−0.25	−0.28	−1.41	0.034	I
D*t*AAg^-Ag^-	0.82	0.59	0.37	0.17	0.09	−0.02	−0.03	0.23	0.034	I
Eg^+ADg^+Eg^+(S7)	0.88	2.59	0.54	3.16	0.59	−1.38	−0.32	−1.71	0.030	VII
D*t*AA*t*Ag^-(S8)	0.98	0.76	0.56	0.06	−0.14	0.09	0.19	0.22	0.025	I

[a] The letter code of each conformation assigned by its φ and ψ backbone angles [40]. The lowercases g^+, t and g^- are used to represent the side-chain torsion angles χ^1 of Cys and Xaa residues. Several local minima were found to have same conformational letter codes, but different side-chain conformations beyond χ^1, leading to different total energies or free energies. The representative conformations are denoted in parentheses.

[b] Relative conformational free energy; $\Delta G_{tot} = \Delta E_{tot} + \Delta\Delta G_{hyd}$.

[c] Relative total conformational energy; $\Delta E_{tot} = \Delta E_{es} + \Delta E_{nb} + \Delta E_{tor} + \Delta E_{cystr} + \Delta E_{loop}$.

[d] Relative electrostatic energy.

[e] Relative nonbonded energy.

[f] Relative torsional energy.

[g] Cystine torsional energy.

[h] Loop energy for the S–S bond.

[i] Hydration free energy change.

[j] Normalized statistical weight calculated by Eq. (1) of the text at $T = 298.15$ K.

[k] β-Turn type for the Pro–Xaa sequence.

This hydrogen bond was also known to be crucial to stabilize the backbone conformations DAAA and DAAC, as noted above. The cyclic CPGC and CPSC peptides have another hydrogen bond between the C=O of Pro residue and the N–H of –NHMe end-group with the distance r(N–H···O) equal to 2.28 and 2.22 Å, respectively.

Populations of backbone conformations for cyclic CPXC peptides in the hydrated state are shown in Fig. 1. For each of cyclic CPXC peptides, populations of 18 backbone conformations are calculated by summing their statistical weights irrespective of conformations for side-chains. The 18 representative backbone conformations are selected, for each of which at lowest one of cyclic CPXC peptides has a statistical weight larger than 0.01.

As expected from the analysis of lowest free energy conformations above, the backbone conformation DAAA is the most preferred for most of cyclic CPXC peptides with statistical weights of 0.314 (X=Gly) to 0.586 (X=Asn) except for the cyclic CPFC peptide. The second preferred backbone conformation is DAAC for most of cyclic CPXC peptides with statistical weights of 0.237 (X=Ala and Ser) to 0.405 (X=Tyr) except for cyclic CPAibC and CPFC peptides. The conformation DCA*C is the second preferred conformation of the CPAibC peptide with a statistical weight of 0.276. It should be noted that both conformations DAAA and DAAC are almost equally feasible for cyclic CPFC and CPYC peptides. The backbone conformation DABA is found to be the third preferred conformation for cyclic CPAC, CPGC, CPFC and CPSC peptides with statistical weights greater than 0.1. In particular, the conformation DABC is the third preferred conformation for the cyclic CPYC peptide with a statistical weight of 0.143.

The analysis of low free energy conformations indicates that the hydrogen bond between the C=O of Cys1 residue and the N–H of Cys4 residue

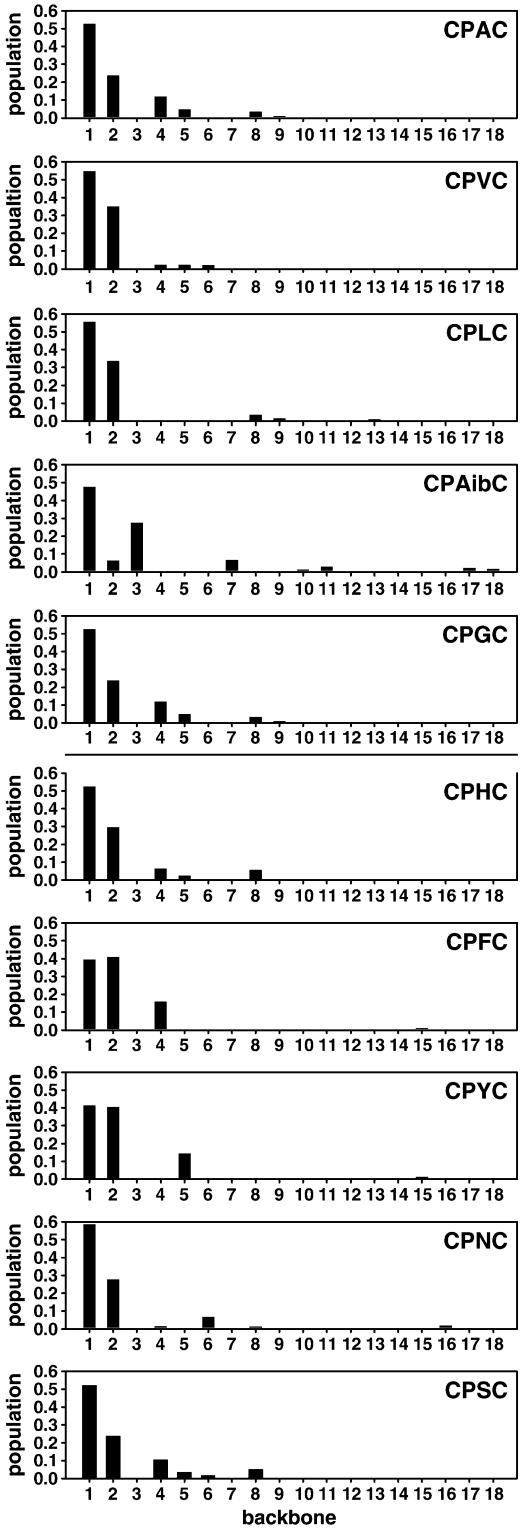

plays a role in stabilizing these preferred backbone conformations. The hydrogen bond distance of r(N–H···O) ranges between 1.96 and 2.01 Å for conformations DAAA and DAAC, whereas the corresponding distance is 2.00–2.10 Å for conformations DABA and DABC. The conformation DCA*C of the cyclic CPAibC peptide has a somewhat longer distance of 2.24 Å. However, it cannot be ruled out that the extended backbone conformations E or F for two Cys residues are also energetically feasible for cyclic CPXC peptides in water by peering the distributions of backbone conformations, as shown in Fig. 1.

However, it should be noted that the most crucial factor to stabilize the overall conformation of cyclic CPXC peptides is the disulfide bond between two cystine residues. The higher propensity of the conformation DAAA for all cyclic CPXC peptides irrespective of the X residue may support this interpretation. By analyzing the low free energy conformations with preferred backbone conformations, it is known that the right-handed disulfide bond prevails with the torsion angle χ_{SS} equal to approximately $+90°$. For the backbone conformations DAAA and DAAC, the values of χ_{SS} are $+66.1°$ to $+75.4°$ and $+71.0°$ to $+76.1°$, respectively, whereas the corresponding values are $+66.8°$ to $+77.3°$ for the conformation DABA. There is only the left-handed disulfide bond with the $\chi_{SS} = -81.6°$ for the second preferred conformation DCA*C of the cyclic CPAibC peptide. Nevertheless, all the bond length of the disulfide bond S–S is calculated to be approximately 2.0 Å.

3.3. Population of β-turns

Although three β-turns can be defined for each of cyclic Ac–CPXC–NHMe peptides, the population of β-turns at the Pro–Xaa sequence is described in detail. The probabilities of occurrence of β-turns for cyclic CPXC peptides in the unhy-

Fig. 1. Population of backbone conformations for cyclic CPXC peptides in the hydrated state. Backbone conformations represented by serial numbers of 1–18 correspond to DAAA, DAAC, DCA*C, DABA, DABC, EAEE, ECA*C, EADE, DACD, ECA*F, DCA*F, DCD*C, DACE, ECB*C, EABC, EAED, A*CA*C and DCA*A, respectively.

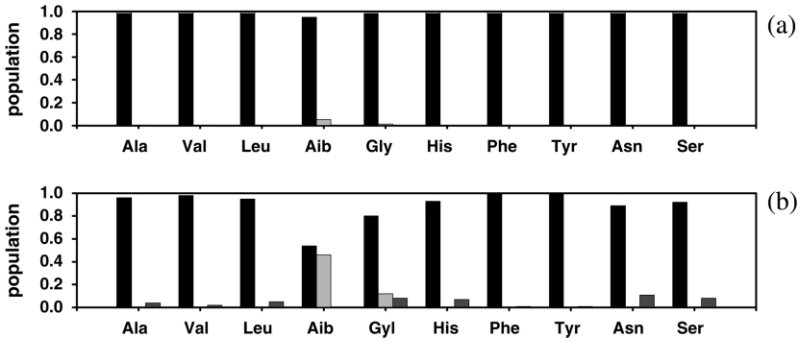

Fig. 2. Population of β-turns at the Pro–Xaa sequence for cyclic CPXC peptides in the unhydrated (a) and hydrated (b) states. The first (black), second (light gray) and third (dark gray) histograms for each peptide correspond to the β-turns of types I, II and VII, respectively.

drated and hydrated states are shown in Fig. 2. In the unhydrated state, the dominant β-turn at the Pro–Xaa sequence is the type I for all cyclic CPXC peptides which has the backbone conformations AA or AB for the Pro–Xaa sequence. These conformations are stabilized by the hydrogen bond between the C=O of Cys1 residue and the N–H of Cys4 residue with a distance of r(N–H···O) equal to 2.0 Å or less, as mentioned in the previous section.

However, the population of type I β-turns of for all CPXC peptides is decreased and that of type VII β-turns is increased in the hydrated state except for the cyclic CPAibC peptide. The increase for type VII β-turns appears to be due to the favored hydration of extended conformations E or F for two Cys residues. For cyclic CPFC and CPYC peptides, the population of type VII β-turns is calculated to be approximately 1%.

In particular, the population of type II β-turns is increased to be 0.456 and 0.120 for the cyclic CPAibC and CPGC peptides, respectively. The backbone conformations for Pro–Aib or Pro–Gly sequences with type II β-turns are CA*, CD*, or CB*. Although, these backbone conformations have the same hydrogen bond between the C=O of Cys1 residue and the N–H of Cys4 residue as the conformations AA or AB with type I β-turns, the hydrogen bond distance r(N–H···O) of the type II is somewhat longer than that of the type I. For example, the hydrogen bond distance is 2.01 Å for the lowest free energy conformation DAAA (B1) with a type I β-turn, whereas the distance is 2.24 Å for the second lowest free energy conformation DCA*C (B2) with a type II β-turn. It should be noted that the relative conformational energy is 2.50 kcal/mol for the conformation DCA*C of the CPAibC peptide in the unhydrated state, whereas its relative total free energy becomes 0.34 kcal/mol in the hydrated state, to which the hydration free energy contributes by −2.24 kcal/mol (Table 2). It seems that the less tighten hydrogen bond may provide better hydration for the polar oxygen of C=O and the hydrogen of N–H.

3.4. Comparison with X-ray and NMR structures of peptides

The X-ray structures of cyclic Ac–CPVC–NHMe [6], Ac–CPSC–NHMe [6] and Boc–CPAibC–NHMe [8] indicate that their preferred backbone conformations are DAAA with type I β-turns for the Pro–Xaa sequence at positions 2 and 3, and with right-handed disulfide bonds, i.e. the torsion angles of χ_{SS} = 78, 70 and 82°, respectively. These X-ray structures are consistent with our calculated lowest free energy conformations in the hydrated state (Table 2), for which calculated values of χ_{SS} are 69, 70 and 66°, respectively. The hydrogen bonds between the C=O of Cys1 residue and the N–H of Cys4 residue appear to play a role in stabilizing type I β-turns of X-ray structures for cyclic CPVC [6], CPSC [6] and CPAibC [8]

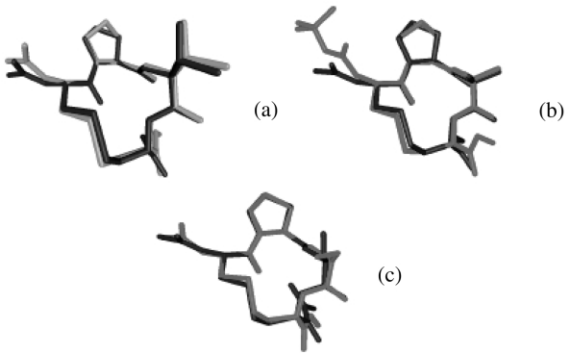

Fig. 3. Superposition of computed lowest free energy conformations of cyclic CPXC peptides in the hydrated state (black) with their X-ray structures (gray): (a) X=Val; (b) X=Aib and (c) X=Ser.

peptides, whose distances of r(N–H···O) are 2.97, 3.07 and 2.94 Å, respectively, whereas our calculated values are 2.86, 2.89 and 2.87 Å for their lowest free energy conformations, respectively. The differences in torsion angles χ_{SS} and hydrogen bond distances may be partially ascribed to the rigid geometry adopted for each residue in calculating conformational energies [49]. The lowest free energy conformations of cyclic CPVC, CPAibC and CPSC peptides (black) are superposed with their X-ray structures (gray) in Fig. 3.

According to ^{1}H NMR assignments for the cyclic Ac–CPSC–NHMe peptide in 90% H_2O/10% D_2O, the major conformation in solution is very similar to the conformation adopted by the peptide in the solid state [6]. The pattern of NOEs and the small temperature dependence of the chemical shift of the N–H of Cys4 residue for the cyclic Ac–CPGC–NHMe peptide was interpreted as the existence of a type II β-turn for Pro and Gly at positions 2 and 3 for a β-turn [6]. In addition, ^{1}H NMR studies on cyclic Boc–CPXC–NHMe peptides (X=Ala, Val, Leu, Aib, Gly, Phe and Tyr) in $CDCl_3$ and/or $(CD_3)_2SO$ indicate the formation of type I β-turns for Pro–Xaa sequences [7–10]. For the CPAibC peptide, the possibility to form a type II β-turn was also proposed [8].

Therefore, our calculated probabilities to form β-turns for all cyclic CPXC peptides may confirm the dominant population of type I β-turns in solution. In particular, the plausible existence of type II β-turns for cyclic CPAibC and CPGC peptides is supported by our calculations. The calculated ^3J coupling constants for cyclic Ac–CPXC–NHMe peptides are listed in Table 3 and compared to experimental values. The calculated values of $^3J_{HN\alpha}$ for Cys1 and Cys4 residues are reasonably consistent with experimental values of Boc–CPXC–NHMe in $(CD_3)_2SO$ and a mixture of $CDCl_3$ and $(CD_3)_2SO$ [7,9,10], whereas the values of $^3J_{HN\alpha}$ for X residues appear to be somewhat underestimated by 1.2–3.5 Hz. The differences in N-terminal end groups and solvents might be factors to bring the discrepancy between calculated and experimental coupling constants.

3.5. Comparison with X-ray protein structures

Richardson examined the types of backbone conformation found at the ends of disulfides in proteins and found that β-turns are to some extent favored at the end of a right-handed disulfide bond [1]. Thornton investigated the β-turn propensity of the sequences of proteins with half-cystines separated by less than four residues and found a strong preference of a right-handed disulfide bond for tetrapeptides to hexapeptides with the higher propensity to form a β-turn [50].

The CPXC sequence is known to be a motif located at active sites of several disulfide oxidoreductases. X-ray structures of oxidoreductases such as thioltransferase (X=Phe) [23], DsbA (X=His) [25], the DsbA homolog (TcpG; X=His) [26], DsbA mutants (X=Tyr, Leu and Ser) [24], and the hyperthermostable oxsidoreductase from *Pyrococcus furiosus* (X=Tyr) [27] do not show significant differences in their conformations of active sites, which have right-handed disulfide bonds with the torsion angle χ_{SS} of approximately +80°. These structural studies exhibit that the Cys1 residue of the active site is located in a loop between β-strand and α-helix, while the Cys4 residue is in the first turn of the α-helix.

The backbone conformation is DAAA for the X-ray structures of the CPFC sequence of thioltransferase [23] and the CPYC sequence of hyperthermostable oxidoreductase [27], whereas it is CAAA for other CPXC sequences (i.e. X=Leu,

Table 3
Coupling constants of cyclic Ac–Cys–Pro–Xaa–Cys–NHMe peptides in the unhydrated and hydrated states

Xaa	State	Cys1			Pro2		Xaa3			Cys4		
		$^3J_{HN\alpha}$	$^3J_{\alpha\beta2}$	$^3J_{\alpha\beta3}$	$^3J_{\alpha\beta2}$	$^3J_{\alpha\beta3}$	$^3J_{HN\alpha}$	$^3J_{\alpha\beta2}$	$^3J_{\alpha\beta3}$	$^3J_{HN\alpha}$	$^3J_{\alpha\beta2}$	$^3J_{\alpha\beta3}$
Calculated												
Ala	Unh	8.0	3.3	12.7	2.5	8.8	5.7	3.4	0.0	6.5	12.8	3.1
	Hyd	8.0	3.3	12.4	2.5	8.8	6.1	3.4	0.0	6.7	12.5	2.9
Val	Unh	7.7	3.2	12.6	2.5	8.8	5.8	0.0	11.6	6.6	12.9	3.2
	Hyd	7.7	3.2	12.4	2.5	8.8	6.0	0.0	11.7	6.7	12.6	3.1
Leu	Unh	7.7	3.3	12.6	2.5	8.8	5.6	8.1	8.0	6.6	12.8	3.2
	Hyd	7.7	3.3	12.3	2.5	8.8	6.0	9.2	7.0	6.8	12.5	3.0
Aib	Unh	8.1	3.1	12.4	2.5	8.8		3.4	3.9	6.7	12.7	3.7
	Hyd	8.0	2.5	11.5	2.5	8.8		4.0	3.2	6.8	12.8	3.4
Gly	Unh	7.6	3.3	12.6	2.5	8.8	5.6			6.8	12.8	3.1
	Hyd	7.6	3.3	11.6	2.5	8.8	5.8			7.0	12.0	2.9
His	Unh	7.7	3.4	11.9	2.5	8.8	6.7	6.5	4.6	6.6	12.6	2.8
	Hyd	7.7	3.4	12.0	2.5	8.8	6.1	8.6	6.7	6.8	12.4	2.9
Phe	Unh	7.6	3.4	12.5	2.5	8.8	6.6	10.5	5.9	6.8	12.8	2.8
	Hyd	7.7	3.4	12.5	2.5	8.8	6.9	11.4	5.2	7.0	12.7	2.7
Tyr	Unh	7.7	3.4	12.3	2.5	8.8	6.7	10.4	6.0	6.7	12.7	2.8
	Hyd	7.7	3.4	12.5	2.5	8.8	7.0	11.2	5.4	6.9	12.6	2.6
Asn	Unh	7.6	3.3	12.4	2.5	8.8	6.2	8.5	3.9	6.5	12.8	3.0
	Hyd	7.5	3.3	11.7	2.5	8.8	5.9	11.1	4.9	6.7	12.0	3.0
Ser	Unh	7.6	3.3	12.5	2.5	8.8	5.4	5.8	4.4	6.5	12.8	3.0
	Hyd	7.6	3.3	12.0	2.5	8.8	5.6	6.9	5.2	6.8	12.3	2.9
Experimental[a]												
Ala[b]		9.0					9.0			5.5		
Val[c,d]		7.3, 7.7					10.3, 9.2			7.7, 7.3		
Leu[b]		8.5					9.5			8.0		
Aib[b]		8.5								7.5		
Gly[b]		8.0								7.0		
Phe[c,e]		8.8, 8.8					9.5, 8.1					
Tyr[c,e]		9.5, 8.8					9.5, 8.8			8.1, 6.6		

Units are in Hz.
[a] Experimental data for cyclic Boc–CPXC–NHMe.
[b] Measured in the mixture of $CDCl_3$ and $(CD_3)_2SO$ [9].
[c] Measured in $CDCl_3$ and $(CD_3)_2SO$; the first and second values for each J correspond to those in $CDCl_3$ and $(CD_3)_2SO$, respectively.
[d] Errors in $J = \pm 0.4$ Hz [7].
[e] Errors in $J = \pm 0.4$ Hz [10].

His, Tyr and Ser) of oxidoreductases [24–26]. The average backbone torsion angles of (ϕ, ψ) for Cys1 residues with the conformational letter code C are ($-86°$, $114°$) [24–26], whereas the corresponding values for the conformation D are ($-158°$, $96°$) [23,27]. Our calculated low free energy conformations for cyclic CPXC peptides with the conformation DCCC in the hydrated state indicate the average values to be ($-152°$, $82°$) for the Cys1 residue. In addition, the average values

are (−129°, 77°) for the Cys1 residues of X-ray structures for cyclic Ac–CPVC–NHMe [6], Ac–CPSC–NHMe [6] and Boc–CPAibC–NHMe [8] peptides. Therefore, the difference in backbone conformations of Cys1 residues for short peptides and proteins may imply that the Cys1 residue located at a loop between β-strand and α-helix in proteins is likely to be affected by neighboring residues.

From X-ray structures of cyclic CPXC sequences for peptides [6,8] and proteins [23–27], the average torsion angle χ_{SS} for the disulfide bond is computed to be +77 and +80°, respectively, i.e. a right-handed disulfide bond. On the other hand, it is calculated to be +71° for our lowest free energy conformations of cyclic Ac–CPXC–NHMe peptides in the hydrated state.

Therefore, our calculated lowest free energy conformations for cyclic CPXC peptides are reasonably consistent with X-ray structures of oxidoreductases. The lowest free energy conformations of cyclic CPXC peptides (black) are superposed with the X-ray structures of corresponding sequences of proteins (gray) in Fig. 4. The differences in backbone conformations and torsion angles for the disulfide bond between our calculated lowest free energy conformations and X-ray structures may be partially attributed to the long-range interactions that the isolated short peptides cannot have and/or to the rigid geometry adopted for each residue used for conformational energy calculations [49].

3.6. Structural implications for CPXC motif of proteins

In lowest free energy conformations and X-ray structures of cyclic CPXC peptides, the hydrogen bond between the C=O of Cys1 residue and the N–H of Cys4 residue is found to play a role in stabilizing type I β-turns of peptide backbone, as noted above. In order to figure out whether this hydrogen bond contributes to the local stability of the cyclic CPXC motif of oxidoreductases, the pattern of hydrogen bonds involving the C=O of Cys1 residues has analyzed. X-ray structures of the CPFC sequence of thioltransferase [23] and the CPYC sequence of hyperthermostable oxidoreductase [27] with the backbone conformation DAAA have the hydrogen bond between backbones of two Cys residues. However, this hydrogen bond can or cannot be seen for CPXC motifs of other proteins with the backbone conformation CAAA [24–26]. Therefore, it can be said that the hydrogen bond between two Cys residues is not a crucial factor to stabilize the local structure of the CPXC motif in proteins, although it may partially contribute to its stability.

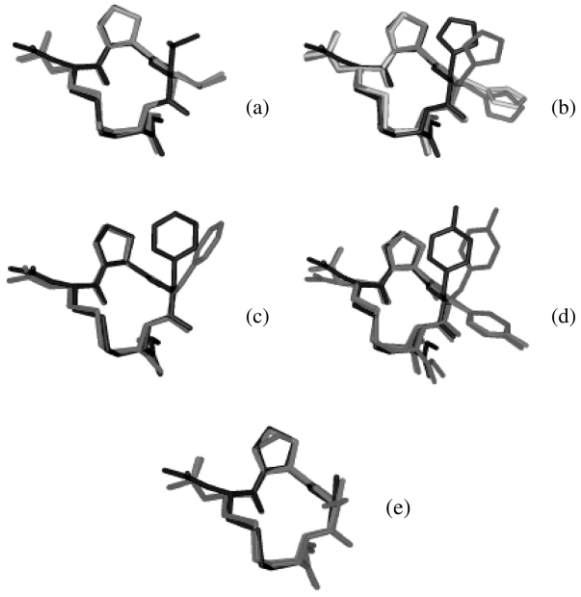

Fig. 4. Superposition of computed lowest free energy conformations DAAA of cyclic CPXC peptides in the hydrated state (black) with the X-ray structures of corresponding sequences of proteins (gray): (a) X=Leu; (b) X=His; (c) X=Phe; (d) X=Tyr and (e) X=Ser.

From the analysis of X-ray structures of proteins, proline is known to be frequently found at the N-terminus of α-helices [29–31]. The higher preference of proline at the beginning of α-helix is suggested to be due to the favored local interactions between two residues preceding proline and no disturbance in hydrogen bonds of α-helix by proline [32]. In fact, each proline of the CPXC motif of oxidoreductases [23–27] considered here is located at the N-terminal of α-helix. Therefore, proline seems to be attributed in stabilizing the local structure of the CPXC motifs.

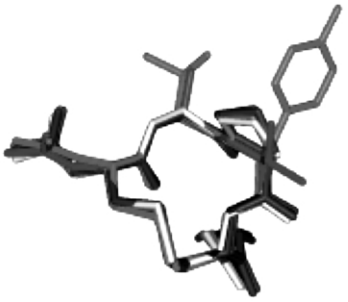

Fig. 5. Superposition of seven X-ray structures of the CXXC sequences for oxidoreductases.

However, X-ray structures of oxidoreductases such as thioredoxins [16,18,19], thioredoxin reductase [21] and T4 glutaredoxin [22] that have no CPXC sequences also show their backbone conformations for the CXXC sequence to be CAAA [16,18,19] or DAAA [21,22], as the same as for CPXC sequences. In Fig. 5, the superposition of X-ray structures of the CXXC sequences for oxidoreductases [16–22] are presented. In particular, thioredoxins have the CPGC sequence and the Gly residue is located at the N-terminal of the α-helix, followed by the Pro residue. It seems that the Pro residue is likely to contribute in stabilizing the α-helix, because the propensity of Pro at the second position of the first turn of α-helix is about a half of that at the N-terminal and cannot be negligible [29–32]. It should, however, be noted that thioredoxin reductase [21] and T4 glutaredoxin [22] have quite similar conformations to thioredoxins, although they have CATC and CVYC sequences, respectively, without any prolines.

Therefore, it can be drawn that the formation of the disulfide bond between two Cys residues of the CPXC motifs in oxidoreductases appears to be crucial in stabilizing the active conformations of the motifs, although the hydrogen bond between two cystines and the Pro residue are likely to contribute to the formation of the β-turn and the first turn of α-helix.

Because of structural similarities in CXXC motifs of oxidoreductases, it is suggested that the reduction potential is determined not only by the XX sequence of active site, but also by noncovalent interactions between the CXXC motif and surrounding residues [15,28,51–53]. In particular, the change in the pK_a of the Cys1 residue of the motif is known to be crucial for the redox properties [15,28]. In each mutant of thioredoxin and DsbA, the lower pK_a of the Cys1 residue is, the more the reduction potential increases [15]. pK_a values of the Cys1 residue of DsbA and its active-site variants are obtained to be 3.28 ± 0.09, 3.75 ± 0.06, 4.42 ± 0.10 and 4.85 ± 0.03 for the XX = PH, PY, PL and PG of the CXXC motif, respectively, from electrochemical experiments [28,52]. According to our calculated results in Table 2, the statistical weights for the lowest free energy conformation DAAA of cyclic CPHC, CPYC, CPLC and CPGC peptides are computed to be 0.229, 0.158, 0.304 and 0.275, respectively. It seems that the intrinsic stability of the cyclic CPXC motif itself for the active conformation might play a role in determining redox properties of proteins.

3.7. Comparison with previous calculations

Oka and co-workers [54–56] have carried out the conformational energy calculations on cyclic Ac–CPXC–NHMe peptides (X = Ala, Val, Leu, Gly and Phe) using an earlier version of the ECEPP force field [57]. They assumed the proline to have the down-puckering with the torsion angle $\phi = -75.0°$, whereas we employed here the up-puckered proline with the torsion angle $\phi = -53.0°$ as well as the revised geometry and nonbonded parameters for proline of the ECEPP/3 force field [35]. It should be noted that X-ray structures of cyclic CPXC sequences of proteins indicate the dominant conformation of proline to be up-puckering [23–27]. In addition, they fixed all torsion angles ω's at 180° during energy minimization and did not take into account the effect of hydration. On the other hand, all torsion angles including ω's are allowed to move during minimization together with including the hydration in this work. A different buildup procedure from ours was adopted to generate starting conformations for energy minimization.

Despite these differences, they found that the backbone conformation DAAA is the lowest energy conformation of cyclic CPXC peptides for X =

Ala, Val, Leu and Phe with a type I β-turn at the Pro–Xaa sequence in the unhydrated state, which accords with our results reported here. The conformation DCA*E was calculated to be the lowest energy conformation of the cyclic CPGC peptide with a type II β-turn, which cannot be found in our low free energy conformations with $\Delta G_{tot} \leqslant 1$ kcal/mol in the hydrated state (Table 2).

4. Conclusions

The backbone conformation DAAA is commonly the most feasible for cyclic CPXC peptides in the hydrated state, which has a type I β-turn at the Pro–Xaa sequence in positions 2 and 3 of a β-turn. The proline residue and the hydrogen bond between backbones of two cystines as well as the formation of disulfide bond appear to play a role in stabilizing this preferred conformation of cyclic CPXC peptides. However, the distributions of backbone conformations and β-turns may indicate that the cyclic CPXC peptide seems to exist as an ensemble of β-turns and coiled conformations in aqueous solution.

Our calculated lowest free energy conformations are consistent with X-ray structures and conformations of cyclic CPXC peptides deduced from NMR experiments as well as X-ray structures of disulfide oxidoreductases. The small conformational differences in backbones and disulfide bonds between calculated and X-ray structures may be partially attributed to the long-range interactions that the isolated short peptides cannot have and/or to the rigid geometry adopted for each residue used for conformational energy calculations.

The structural similarities in CXXC motifs of oxidoreductases may imply that the redox properties are determined not only by the XX sequence of active site, but also by noncovalent interactions between the CXXC motif and surrounding residues. Nevertheless, the intrinsic stability of the cyclic CPXC motif itself for the active conformation appears to play a role in determining electrochemical properties of disulfide oxidoreductases.

References

[1] J.S. Richardson, The anatomy and taxonomy of protein structure, Adv. Protein Chem. 34 (1981) 167–339.

[2] W.J. Wedemeyer, E. Welker, M. Narayan, H.A. Scheraga, Disulfide bonds and protein folding, Biochemistry 39 (2000) 4207–4216, and references therein.

[3] C.N. Pace, G.R. Grimsley, J.A. Thomson, B.J. Barnett, Conformational stability and activity of ribonuclease T_1 with zero, one, and two intact disulfide bonds, J. Biol. Chem. 263 (1988) 11820–11825.

[4] S. Talluri, C.M. Falcomer, H.A. Scheraga, Energetic and structural basis for the preferential formation of the native disulfide loop involving Cys-65 and Cys-72 in synthetic peptide fragments derived from the sequence of ribonuclease A, J. Am. Chem. Soc. 115 (1993) 3041–3047.

[5] G.T. Montelione, H.A. Scheraga, Formation of local structures in protein folding, Acc. Chem. Res. 22 (1989) 70–76, and references therein.

[6] C.M. Falcomer, Y.C. Meinwald, I. Choudhary, et al., Chain reversals in model peptides: studies of cystine-containing cyclic peptides. 3. Conformational free energies of cyclization of tetrapeptides of sequence Ac–Cys–Pro–X–Cys–NHMe, J. Am. Chem. Soc. 114 (1992) 4036–4042.

[7] Y.V. Venkatachalapathi, B.V.V. Prasad, P. Balaram, Conformational analysis of small disulfide loops. Spectroscopic and theoretical studies on a synthetic cyclic tetrapeptide containing cystine, Biochemistry 21 (1982) 5502–5509.

[8] A. Ravi, B.V.V. Prasad, P. Balaram, Cyclic peptide disulfides. Solution and solid-state conformation of Boc–Cys–Pro–Aib–Cys–NHMe, a disulfide-bridged peptide helix, J. Am. Chem. Soc. 105 (1983) 105–109.

[9] A. Ravi, P. Balaram, Stabilization of β-turn conformations in Pro–X sequences by disulfide bridging. Synthesis and solution conformations of five cyclic cystine peptides, Tetrahedron 40 (1984) 2577–2583.

[10] R. Kishore, S. Raghothama, P. Balaram, Synthetic peptide models for the redox-active disulfide loop of glutaredoxin. Conformational Studies, Biochemistry 27 (1988) 2462–2471.

[11] S.S. Zimmerman, H.A. Scheraga, Influence of local interactions on protein structure. I. Conformational energy studies of *N*-acetyl-*N*′-Methylamides of Pro–X and X–Pro dipeptides, Biopolymers 16 (1977) 811–843.

[12] C.M. Wilmot, J.M. Thornton, Analysis and prediction of the different types of β-turn in proteins, J. Mol. Biol. 203 (1988) 221–232.

[13] E.G. Hutchinson, J.M. Thornton, A revised set of potentials for β-turn formation in proteins, Protein Sci. 3 (1994) 2207–2216.

[14] A. Holmgren, Thioredoxin, Annu. Rev. Biochem. 54 (1985) 237–271.

[15] P.T. Chivers, K.E. Prehoda, R.T. Raines, The CXXC motif: a rheostat in the active site, Biochemistry 36 (1997) 4061–4066.

[16] S.K. Katti, D.M. LeMaster, H. Eklund, Crystal structure of thioredoxin from *Escherichia coli* at 1.68 Å resolution, J. Mol. Biol. 212 (1990) 167–184.

[17] M.F. Jeng, A.P. Campbell, T. Begley, et al., High-resolution solution structures of oxidized and reduced *Escherichia coli* thioredoxin, Structure 2 (1994) 853–868.
[18] M. Saarinen, F.K. Gleason, H. Eklund, Crystal structure of thioredoxin-2 from *Anabaena*, Structure 3 (1995) 1097–1108.
[19] G. Capitani, Z. Markovic-Housley, G. DelVal, M. Morris, J.N. Jansonius, P. Schürmann, Crystal structures of two functionally different thioredoxins in spinach chloroplasts, J. Mol. Biol. 302 (2000) 135–154.
[20] T.-H. Xia, J.H. Bushweller, P. Sodano, et al., NMR structure of oxidized *Escherichia coli* glutaredoxin: comparison with reduced *E. coli* glutaredoxin and functionally related proteins, Protein Sci. 1 (1992) 310–321.
[21] G. Waksman, T.S.R. Krishna, C.H. Williams Jr., J. Kuriyan, Crystal structure of *Escherichia coli* thioredoxin reductase refined at 2 Å resolution, J. Mol. Biol. 236 (1994) 800–816.
[22] H. Eklund, M. Ingelman, B.O. Söderberg, et al., Structure of oxidized bacteriophage T4 glutaredoxin (thioredoxin), J. Mol. Biol. 228 (1992) 596–618.
[23] S.K. Katti, A.H. Robbins, Y. Yang, W.W. Wells, Crystal structure of thioltransferase at 2.2 Å resolution, Protein Sci. 4 (1995) 1998–2005.
[24] L.W. Guddat, J.C.A. Bardwell, R. Glockshuber, M. Huber-Wunderlich, T. Zander, J.L. Martin, Structural analysis of three His32 mutants of DsbA: support for an electrostatic role of His32 in DsbA stability, Protein Sci. 6 (1997) 1893–1900.
[25] L.W. Guddat, J.C.A. Bardwell, T. Zander, J.L. Martin, The uncharged surface features surrounding the active site of *Escherichia coli* DsbA are conserved and are implicated in peptide binding, Protein Sci. 6 (1997) 1148–1156.
[26] S.H. Hu, J.A. Peek, E. Rattigan, R.K. Taylor, J.L. Martin, Structure of TcpG, the DsbA protein folding catalyst from *Vibrio cholerae*, J. Mol. Biol. 268 (1997) 137–146.
[27] B. Ren, G. Tibbelin, D. de Pascale, M. Rossi, S. Bartolucci, R. Ladenstein, A protein disulfide oxidoreductase from the archaeon *Pyrococcus furiosus* contains two thioredoxin fold units, Nat. Struct. Biol. 5 (1998) 602–611.
[28] M. Huber-Wunderlich, R. Glockshuber, A single dipeptide sequence modulates the redox properties of a whole enzyme family, Fold. Des. 3 (1998) 161–171.
[29] J.S. Richardson, D.C. Richardson, Amino acid preferences for specific locations at the ends of α-helices, Science 240 (1988) 1648–1652.
[30] R. Aurora, G.D. Rose, Helix capping, Protein Sci. 7 (1998) 21–38.
[31] S. Kumar, M. Bansal, Dissecting α-helices: position-specific analysis of α-helices in globular proteins, Proteins Struct. Funct. Genet. 31 (1998) 460–476.
[32] M.K. Kim, Y.K. Kang, Positional preference of proline in α-helices, Protein Sci. 8 (1999) 1492–1499.
[33] IUPAC-IUB Commission on biochemical nomenclature, Abbreviations and symbols for the description of the conformation of polypeptide chains, Biochemistry 9 (1970) 3471–3479.
[34] IUPAC-IUB Joint commission on biochemical nomenclature, Nomenclature and symbolism for amino acids and peptides, J. Biol. Chem. 260 (1985) 14–42.
[35] G. Némethy, K.D. Gibson, K.A. Palmer, et al., Energy parameters in polypeptides. 10. Improved geometrical parameters and nonbonded interactions for use in the ECEPP/3 algorithm, with application to proline-containing peptides, J. Phys. Chem. 96 (1992) 6472–6484.
[36] Y.K. Kang, G. Némethy, H.A. Scheraga, Free energies of hydration of solute molecules. 1. Improvement of the hydration shell model by exact computations of overlapping volumes, J. Phys. Chem. 91 (1987) 4105–4109.
[37] Y.K. Kang, G. Némethy, H.A. Scheraga, Free energies of hydration of solute molecules. 2. Application of the hydration shell model to nonionic molecules, J. Phys. Chem. 91 (1987) 4109–4117.
[38] Y.K. Kang, G. Némethy, H.A. Scheraga, Free energies of hydration of solute molecules. 3. Application of the hydration shell model to charged organic molecules, J. Phys. Chem. 91 (1987) 4118–4120.
[39] Y.K. Kang, K.D. Gibson, G. Némethy, H.A. Scheraga, Free energies of hydration of solute molecules. 4. Revised treatment of the hydration shell model, J. Phys. Chem. 92 (1988) 4739–4742.
[40] S.S. Zimmerman, M.S. Pottle, G. Némethy, H.A. Scheraga, Conformational analysis of the 20 naturally occurring amino acid residues using ECEPP, Macromolecules 10 (1977) 1–9.
[41] E.J. Milner-White, L.H. Bell, P.H. Maccallum, Pyrrolidine ring puckering in *cis* and *trans*-proline residues in proteins and polypeptides, J. Mol. Biol. 228 (1992) 725–734.
[42] M. Vásquez, G. Némethy, H.A. Scheraga, Computed conformational states of the 20 naturally occurring amino acid residues and of the prototype residue α-aminobutyric acid, Macromolecules 16 (1983) 1043–1049.
[43] M. Vásquez, H.A. Scheraga, Use of buildup and energy-minimization procedures to compute low-energy structures of the backbone of enkephalin, Biopolymers 24 (1985) 1437–1447.
[44] K.D. Gibson, H.A. Scheraga, Revised algorithms for the build-up procedure for predicting protein conformations by energy minimization, J. Comput. Chem. 8 (1987) 826–834.
[45] D.M. Gay, Subroutines for unconstrained minimization using a model/trust-region approach, ACM Trans. Math. Software 9 (1983) 503–524.
[46] G. Némethy, H.A. Scheraga, Stereochemical requirements for the existence of hydrogen bonds in β-bends, Biochem. Biophys. Res. Commun. 95 (1980) 320–327.
[47] A. Pardi, M. Billeter, K. Wüthrich, Calibration of the angular dependence of the amide proton-C^{α} proton

coupling constants, $^{3}J_{HN\alpha}$, in a globular protein: use of $^{3}J_{HN\alpha}$ for identification of helical secondary structure, J. Mol. Biol. 180 (1984) 741–751.
[48] A. DeMarco, M. Llinás, K. Wüthrich, Analysis of the ^{1}H-NMR spectra of ferrichrome peptides. I. The non-amide protons, Biopolymers 17 (1978) 617–636.
[49] P.A. Karplus, Experimentally observed conformation-dependent geometry and hidden strain in proteins, Protein Sci. 5 (1996) 1406–1420.
[50] J.M. Thornton, Disulphide bridges in globular proteins, J. Mol. Biol. 151 (1981) 261–287.
[51] H. Eklund, F.K. Gleason, A. Holmgren, Structural and functional relations among thioredoxins of different species, Proteins Struct. Funct. Genet. 11 (1991) 13–28.
[52] U. Grauschopf, J.R. Winther, P. Korber, T. Zander, P. Dallinger, J.C.A. Bardwell, Why is DsbA such an oxidizing disulfide catalyst?, Cell 83 (1995) 947–955.
[53] J.B. Charbonnier, P. Belin, M. Moutiez, E.A. Stura, E. Quéméneur, On the role of the cis-proline residue in the active site of DsbA, Protein Sci. 8 (1999) 96–105.
[54] J. Yoshimoto, A. Nishinaga, M. Oka, T. Hayashi, Theoretical conformational analysis of tetrapeptide Ac–Cys–Pro–Gly–Cys–NHMe with disulfide linkage, Polym. Bull. 38 (1997) 109–115.
[55] J. Yoshimoto, A. Nishinaga, M. Oka, T. Hayashi, Theoretical conformational analysis of tetrapeptide Ac–Cys–Pro–Ala–Cys–NHMe with disulfide linkage, Polym. Bull. 38 (1997) 227–234.
[56] Y. Ishikawa, Y. Hirano, J. Yoshimoto, M. Oka, T. Hayashi, Theoretical conformational analysis of disulfide-linked tetrapeptides Ac–Cys–Pro–Xaa–Cys–NHMe having hydrophobic Xaa amino-acid residues, Polym. J. 30 (1998) 256–261.
[57] F.A. Momany, R.F. McGuire, A.W. Burgess, H.A. Scheraga, Energy parameters in polypeptides. VII. Geometric parameters, partial atomic charges, nonbonded interactions, hydrogen bond interactions, and intrinsic torsional potentials for the naturally occurring amino acids, J. Phys. Chem. 79 (1975) 2361–2381.